Biomaterials 32 (2011) 5706–5716

Contents lists available at ScienceDirect

Biomaterials

journal homepage: www.elsevier.com/locate/biomaterials

Antibacterial nano-structured titania coating incorporated with silver nanoparticles

Lingzhou Zhao [a,c,1], Hairong Wang [b,1], Kaifu Huo [b,c,*], Lingyun Cui [a], Wenrui Zhang [b], Hongwei Ni [b], Yumei Zhang [a], Zhifen Wu [a], Paul K. Chu [c,*]

[a] School of Stomatology, The Fourth Military Medical University, No. 145 West Changle Road, Xi'an 710032, China
[b] School of Materials and Metallurgy, Wuhan University of Science and Technology, Wuhan 430081, China
[c] Department of Physics and Materials Science, City University of Hong Kong, Tat Chee Avenue, Kowloon, Hong Kong, China

ARTICLE INFO

Article history:
Received 1 April 2011
Accepted 18 April 2011
Available online 12 May 2011

Keywords:
Titania nanotubes
Ag nanoparticles
Antibacterial properties
Osteoblasts
Cytotoxicity

ABSTRACT

Titanium (Ti) implants are widely used clinically but post-operation infection remains one of the most common and serious complications. A surface boasting long-term antibacterial ability is highly desirable in order to prevent implant associated infection. In this study, titania nanotubes (TiO_2-NTs) incorporated with silver (Ag) nanoparticles are fabricated on Ti implants to achieve this purpose. The Ag nanoparticles adhere tightly to the wall of the TiO_2-NTs prepared by immersion in a silver nitrate solution followed by ultraviolet light radiation. The amount of Ag introduced to the NTs can be varied by changing processing parameters such as the $AgNO_3$ concentration and immersion time. The TiO_2-NTs loaded with Ag nanoparticles (NT-Ag) can kill all the planktonic bacteria in the suspension during the first several days, and the ability of the NT-Ag to prevent bacterial adhesion is maintained without obvious decline for 30 days, which are normally long enough to prevent post-operation infection in the early and intermediate stages and perhaps even late infection around the implant. Although the NT-Ag structure shows some cytotoxicity, it can be reduced by controlling the Ag release rate. The NT-Ag materials are also expected to possess satisfactory osteoconductivity in addition to the good biological performance expected of TiO_2-NTs. This controllable NT-Ag structure which provides relatively long-term antibacterial ability and good tissue integration has promising applications in orthopedics, dentistry, and other biomedical devices.

1. Introduction

Titanium (Ti) implants are widely used clinically, but implant associated infection remains one of the most serious complications and is usually difficult to treat sometimes requiring implant removal and repeated surgeries [1,2]. Although various measures such as thorough disinfection and stringent aseptic surgical protocols have been proposed to mitigate bacterial contamination, bacterial invasion usually occurs after surgery [3] and complications can also arise from infection of nearby tissues or a hematogenous source at a later time [4]. Different implant materials respond differently to bacteria attack due to their structures and properties. For instance, for percutaneous external fixation pins and transmucosal dental implants [5], bacteria on the adjacent skin, mucosa, and implant surface can invade through the soft tissue/implant interface. Generally and collectively, implants are vulnerable to bacterial invasion throughout their lifetime and so it is important to attain long-term ability to combat bacterial colonization on the implants in order to maintain normal functions. The main reason for the high incidence of implant associated infection and difficult treatment is that the adhered bacteria form a biofilm which makes the bacteria highly resistant to the host defense and antimicrobial therapy [6,7]. Besides, the topical host defense is compromised by surgical trauma and implant insertion further facilitating bacteria invasion. It is generally accepted that the most effective method to prevent biofilm buildup on implants is to prohibit initial bacterial adhesion since biofilms are hard to remove after formation [1,6]. Although antibacterial coatings have been widely explored to prevent biofilm formation, attempts to fabricate ones with long-term antibacterial capability are relatively scarce, but there is growing interest in incorporating antibacterial agents

* Corresponding authors. Department of Physics and Materials Science, City University of Hong Kong, Tat Chee Avenue, Kowloon, Hong Kong, China. Tel.: +1 852 27887724; fax: +1 852 27889549.
E-mail addresses: kfhuo@wust.edu.cnor, kaifuhuo@cityu.edu.hk (K. Huo), paul.chu@cityu.edu.hk (P.K. Chu).
[1] These two authors contribute equally to this work.

0142-9612/$ – see front matter © 2011 Elsevier Ltd. All rights reserved.
doi:10.1016/j.biomaterials.2011.04.040

into coatings on biomedical implants. By optimizing the structure as well as antibacterial agent loading capacity and release rate, materials that possess more long-term antibacterial ability and promote tissue integration and repair simultaneously may be produced.

Since bone tissues are composed of hierarchical nano-composites, the proper nanotopography can promote osteo-conductivity from the biomimetic viewpoint. As a result, surface modification of biomaterials including surface nanotexturing has been explored extensively [8–18]. In particular, highly ordered titania nanotubes (TiO_2-NTs) fabricated on Ti implants by electrochemical anodization have attracted increasing attention [11–18]. TiO_2-NTs have a lower elastic modulus of approximately 36–43 GPa [17] which is much closer to that of natural bones and are expected to have better biomechanical compatibility than other artificial biomaterials. For instance, TiO_2-NTs have been found to foster the growth of nano-structured hydroxyapatite in simulated body fluids [13] and induce extracellular matrix secretion, mineralization, and other functions of bone cells [12,14–16]. Moreover, our recent study revealed that the hierarchical hybrid TiO_2 micropits/nanotubes structures induced more balanced promotion of multiple cell functions [11]. Therefore, TiO_2-NTs are promising bioactive coatings that can induce direct bone-implant bonding with enhanced host defense on the implant surface.

Another merit of TiO_2-NTs is that they can serve as carriers for drugs such as antibacterial agents [18,19] and it opens up the possibility of long-term antibacterial functionality as aforementioned. Various kinds of antibiotics have been studied but in spite of scattered success, development of new antibiotics resistant strains after prolonged use reduces the effectiveness [20–24]. Silver (Ag) is one of the strong bactericides and has attracted increasing attention because of other benefits such as a broad antibacterial spectrum including antibiotic-resistant bacteria, non-cytotoxicity at suitable doses, satisfactory stability, and smaller possibility to develop resistant strains [1,3,24–29]. Since the required Ag dose is typically low, it is possible to fabricate coatings with long-term antibacterial characteristics by introducing and controlling Ag release. In fact, it has been reported that a certain range of Ag concentrations can kill bacteria without impairing mammalian cell functions [24] and Ag-containing coatings that can resist biofilm formation and do not show cytotoxicity have been explored [3,24,26,28].

We believe that by optimizing the structure of TiO_2-NTs from the perspective of tissue integration, introducing a sufficient amount of Ag, and regulating the Ag release rate in a controlled manner, a surface that boasts a relatively long-term antibacterial ability and simultaneously enhances cell functions can be produced. In this study, we investigate whether Ag can be incorporated into TiO_2-NTs controllably and reliably and if the Ag loaded TiO_2-NTs (NT-Ag) indeed possess long-term antibacterial capability and other desirable biological functionalities.

2. Materials and methods

2.1. Specimen preparation

Pure titanium foils (Aldrich, 10 × 10 × 1 mm^3) underwent electrochemical anodization to form a titania nanotubular layer. The Ti foils were polished by SiC sandpapers and then ultrasonically cleaned with acetone, ethanol, and deionized water sequentially. Anodization was carried out in a conventional two-electrode cell equipped with a direct current (DC) power supply (IT6834, ITECH, China). The Ti foil served as the anode electrode and a graphite foil as the counter electrode (1 cm separation). The electrolyte was ethylene glycol containing 0.5 wt % ammonium fluoride (NH_4F) and 5 vol % distilled (DI) water. After anodization at 60 V for 1 h, TiO_2-NTs were formed on Ti foils. The samples were ultrasonically cleaned and annealed at 450 °C in air for 3 h to convert the amorphous TiO_2-NTs into the anatase phase. The annealed samples were soaked in $AgNO_3$ solutions with four different concentrations (0.5, 1, 1.5 and 2 M) for 10 min. Afterward, they were rinsed with deionized water, dried, and irradiated with UV light from a high-pressure Hg lamp for 10 min. This process was carried out once for the 0.5 M group and twice for the 1, 1.5 and 2 M samples to obtain NT-Ag samples with different Ag contents.These samples were denoted as NT-Ag0.5, NT-Ag1.0, NT-Ag1.5 and NT-Ag2.0, respectively. After ultrasonic cleaning (3 times and 10 min each), both sides of the samples were sterilized by UV irradiation for 30 min before ensuing antibacterial and cell culture experiments.

2.2. Surface characterization

Field-emission scanning electron microscopy (FE-SEM, FEI Nova 400 Nano) and atomic force microscopy (AFM, Auto-Probe CP, Park Scientific Instruments) were utilized to determine the surface topography of the specimens, and transmission electron microscopy (TEM, Philips CM20) was used to observe the microstructure of the Ag loaded nanotubes. The crystalline structure of the samples was determined by X-ray diffraction (XRD, Philips X′ Pert Pro), and the chemical composition of the surface layer was determined by X-ray photoelectron spectroscopy (XPS, ESCALAB MK-II).

2.3. Sliver release

The amounts of Ag released from the NT-Ag samples were monitored in the phosphate buffered saline (PBS). The samples were immersed in 6 ml of PBS for 1 day in dark, taken out, and then immersed again in 6 ml of fresh PBS. This process was repeated for a total of 14 days to generate solutions at different time points in order to determine the Ag release time profile. The PBS solution containing released silver was analyzed by inductively-coupled plasma atomic emission spectrometry (ICP-AES, IRIS Advantage ER/S).

2.4. Antibacterial assay

The antibacterial ability was evaluated using Staphylococcus aureus (S. aureus, ATCC 6538) cultivated in a beef extract-peptone (BEP) medium at 37 °C for 12 h. It was adjusted to a concentration of 10^5 CFU/ml in the antibacterial assay. Each specimen was incubated in 1 ml of the bacteria suspension in BEP at 37 °C for 1 day. At the end of the incubation period, the culture medium was sampled to determine the viable counts of planktonic bacteria. The specimens were gently rinsed thrice with PBS in order to eliminate non-adherent bacteria, and the adhered bacteria on each specimen were detached into 1 ml of BEP by ultrasonic vibration (40 W) for 5 min with the resulting bacterial suspension sampled to count the viable bacteria adhered on the specimens. Complete detachment of the adhered bacteria by ultrasonic vibration was verified by fluorescence microscopy after fluorescence staining. Afterward, the specimens were ultrasonically cleaned, dried, sterilized, and re-incubated as described above. This process was repeated daily for a total incubation time of 30 days. The viable bacteria in the sampled suspensions at days 1, 4, 7, 10, 15, 20, and 30 were counted by serial dilution and the spread plate method. The antibacterial rates with regard to planktonic bacteria in the culture medium and the antibacterial rates for adhered bacteria on the specimens were calculated based on the following formulas: (1) Antibacterial rate for planktonic bacteria in the medium (Rp) (%) $= (B - A)/B \times 100\%$ and (2) Antibacterial rate for adherent bacteria on the specimen (Ra) (%) $= (D - C)/D \times 100\%$. Here, A indicates the average number of viable bacteria in the culture medium inoculated with the specimen, B is the average number of viable bacteria in the culture medium inoculated with no specimen (blank control), C is the average number of viable bacteria on the NT-Ag specimens, and D is the average number of viable bacteria on the TiO_2-NTs.

In order to perform fluorescence staining to show the viability of bacteria on the samples, bacteria were inoculated on the samples mentioned above. The bacteria medium was refreshed every 24 h for a total of 7 days. Afterward, a new bacteria suspension was added and cultured for another 7 h. The culture medium was then removed and the samples were rinsed with PBS, stained using acridine orange and ethidium bromide for 15 min in dark, and observed by fluorescence microscopy (Olympus). Ethidium bromide did not penetrate the plasma membrane in the viable cells and stained only the dead cells, whereas acridine orange penetrated the plasma membrane without permeabilization and stained the viable and dead cells. When examined by fluorescence microscopy, the living cells appeared green while the dead cells were orange.

2.5. Protein adsorption assay

A 1 ml droplet of the Dulbecco's minimum essential medium (DMEM, Gibco) containing 10% bovine calf serum (BCS, Gibco) was pipetted onto each specimen. After incubation at 37 °C for 4 h, the disks were placed in new 24 well plates (one disk per well) and washed with PBS thrice. 500 μl of 1% sodium dodecyl sulfate (SDS) solution was added to these wells and shaken for 1 h to detach proteins from the disk surfaces.The protein concentrations in the collected SDS solutions were determined using a MicroBCA protein assay kit (Pierce).

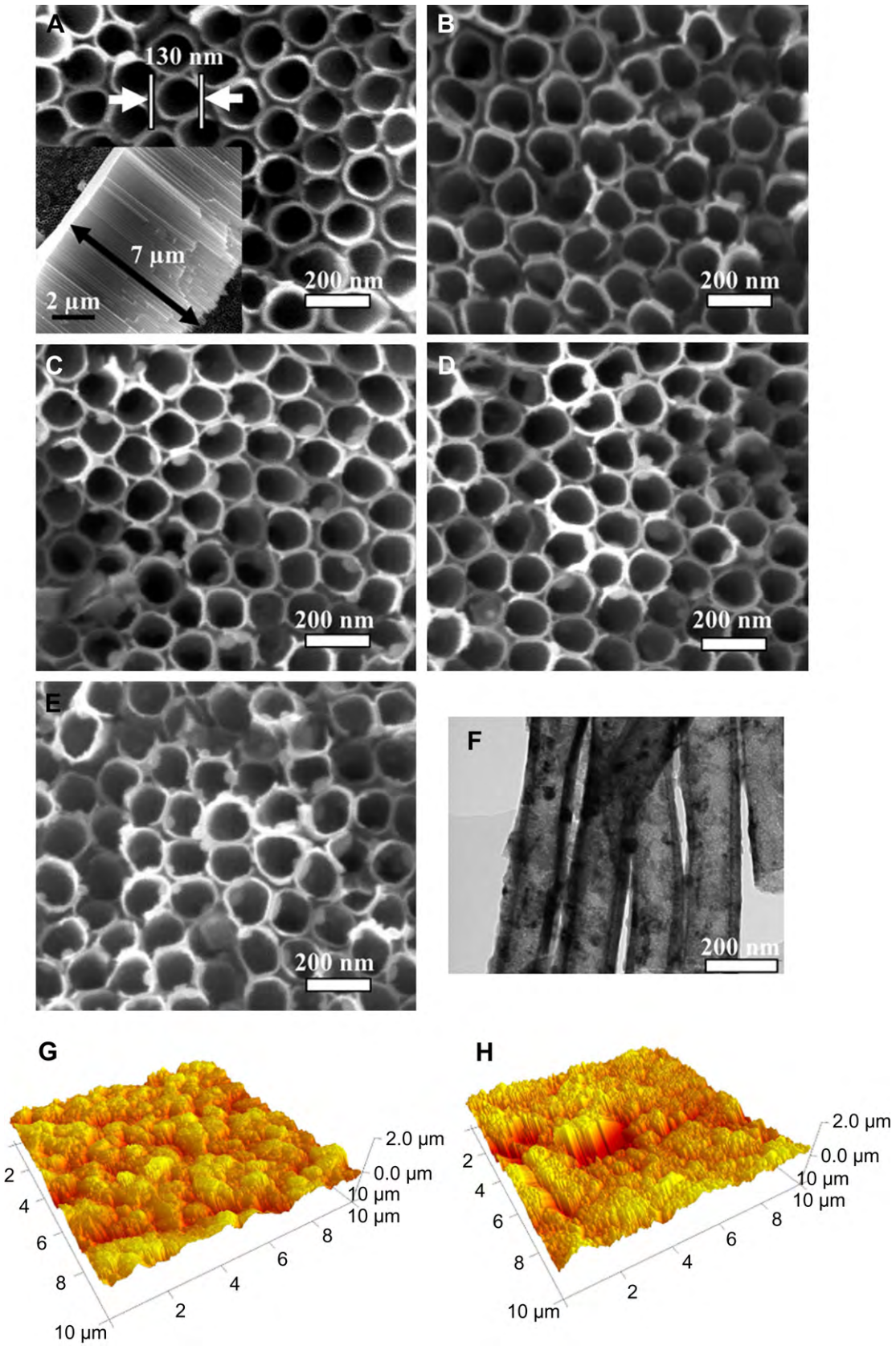

Fig. 1. SEM images of the samples: (A) TiO_2-NTs, (B) NT-Ag0.5, (C) NT-Ag1.0, (D) NT-Ag1.5 and (E) NT-Ag2.0. The inset in (A) is the side-view SEM image revealing that the length of the nanotubes is about 7 μm (F) TEM image of NT-Ag1.0. (G) and (H) AFM images of TiO_2-NTs and NT-Ag1.0, respectively.

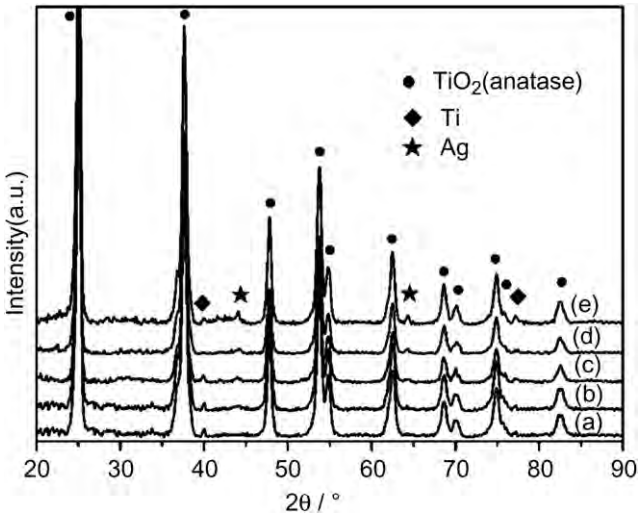

Fig. 2. XRD patterns of samples: (a) TiO_2-NTs, (b) NT-Ag0.5, (c) NT-Ag1.0, (d) NT-Ag1.5 and (e) NT-Ag2.0.

2.6. Cell culture

Primary rat osteoblasts were extracted by digesting the calvarial bone of neonatal Sprague–Dawley rats [30]. The cells were cultured in DMEM containing 10% BCS and 1% penicillin/streptomycin and incubated in a humidified atmosphere of 5% CO_2 at 37 °C. Passages 2–5 were used in the experiments.

2.7. Lactate dehydrogenase activity assay

The activity of lactate dehydrogenase (LDH) in the culture media released by the cells was used as an index of cytotoxicity. After incubation for 1 day, the culture media were sampled and centrifuged, and the supernatant was used for the LDH activity assay. The LDH activity was determined spectrophotometrically according to the manufacturer's instructions (Sigma).

2.8. Cell number

The cells were seeded on the specimens placed in 24 well plates at a density of 2×10^4 cells/well. After culturing for 1 and 4 days, cell numbers were determined by DNA assay as previously reported [31]. Briefly, cells on samples were digested in 500 μl buffer solution (0.5 mg/ml proteinase K (Beyotime), 0.2 mg/ml sodium dodecyl sulfate (Solarbio), and 30 mM saline-sodium citrate (SSC)) at 56 °C overnight. The resulting mixture was subjected to centrifugation and aliquots (50 μl) of the supernatants after mixing with 150 μl Hoechst 33258 dye solution (1 μg/ml, Sigma) and transferred to 96-well plates. The DNA content was quantified spectrofluorometrically using a Multi-Detection microplate reader (Bio-Rad) at a wavelength of 465 nm (excitation wavelength of 360 nm) by correlating with a DNA standard curve which was generated by lysing serial dilution of a known concentration of osteoblasts.

2.9. Intracellular total protein synthesis and alkaline phosphatase activity

A 1 ml cell suspension was seeded on each specimen at a density of 2×10^4 cells/ml. After culturing for 7 days, the cells were washed with PBS and lysed in 0.1 vol% Triton X-100 using the standard freeze–thaw cycles. The alkaline phosphatase (ALP) activity in the lysis was determined by means of a colorimetric assay using an ALP reagent containing p-nitrophenyl phosphate (p-NPP) as the substrate. The absorbance of the formed p-nitrophenol was measured at 405 nm. The intracellular total protein content was determined using the MicroBCA protein assay kit and the ALP activity was normalized to it.

2.10. Statistical analysis

The assays were performed in triplicate and data were expressed as means ± standard deviations. Each experiment was repeated three times with data from a typical experiment shown. A one-way ANOVA combined with a Student-Newman-Keuls (SNK) *post hoc* test was utilized to determine the level of significance. $p < 0.05$ was regarded to be significant and $p < 0.01$ was considered highly significant.

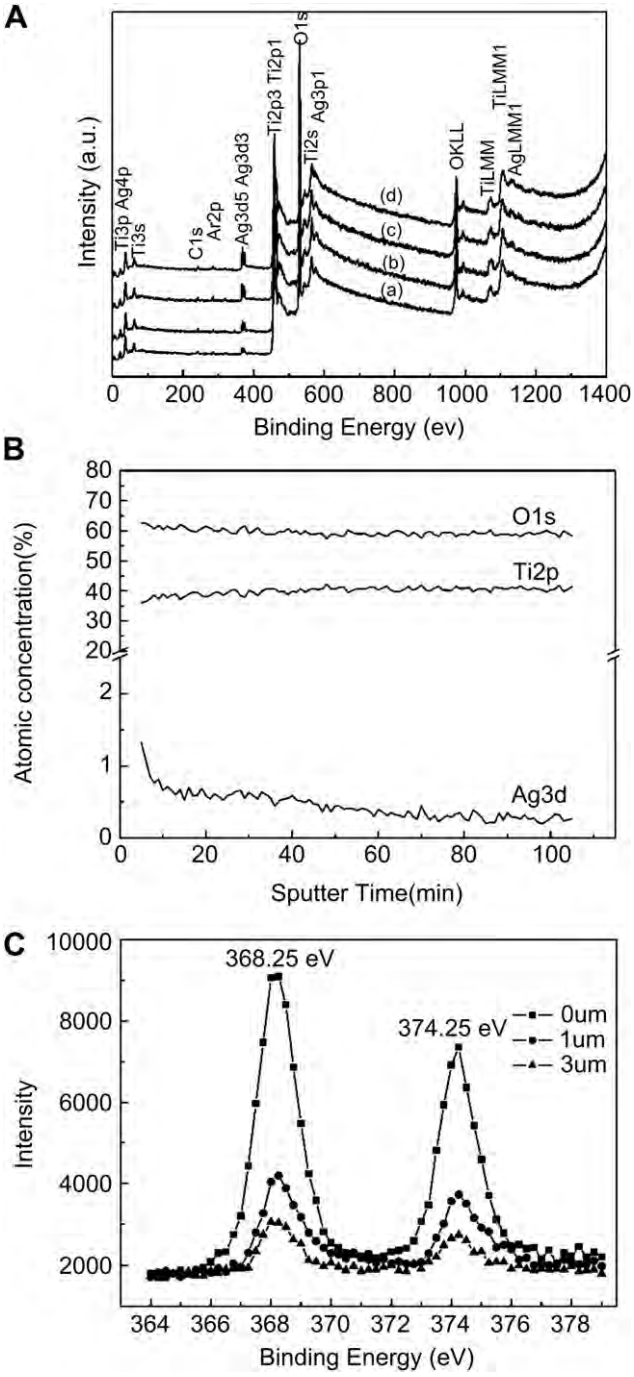

Fig. 3. (A) XPS survey spectra of (a) NT-Ag0.5, (b) NT-Ag1.0, (c) NT-Ag1.5, and (d) NT-Ag2.0, (B) XPS depth profile of sample NT-Ag1.0 using a sputtering rate of 21 nm/min and (C) high-resolution XPS spectra of Ag3d at different depths in NT-Ag1.0.

3. Results

3.1. Surface characterization

The SEM and AFM pictures of the TiO_2-NTs and the NT-Ag samples as well as TEM images of the nanotubes taken from NT-Ag1.0 are depicted in Fig. 1. The TiO_2-NTs formed by anodization of a Ti foil at 60 V for 1 h have a typical diameter of about 130 nm and length of about 7 μm (Fig. 1A). Fig. 1B–E display the SEM images of NT-Ag0.5, NT-Ag1.0, NT-Ag1.5, and NT-Ag2.0, respectively. The NT-Ag samples retain the nanotubular structure with Ag

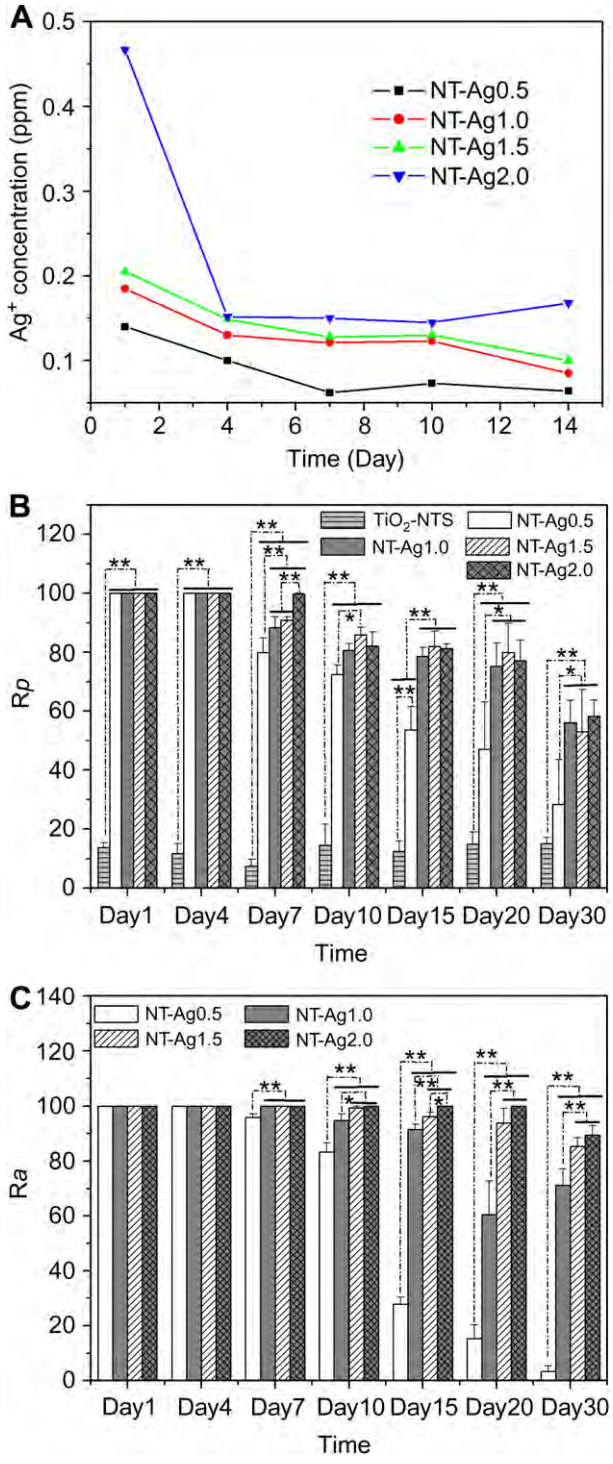

Fig. 4. (A) Non-cumulative silver release profiles from NT-Ag into PBS, (B) Antibacterial rates against planktonic bacteria in the medium (R*p*), and (C) Antibacterial rates against adherent bacteria on the specimen (R*a*). The antibacterial assays data are expressed as means ± standard deviations ($n = 3$). One-way ANOVA followed by SNK *post hoc* test is utilized to determine the level of significance. $^{*}p < 0.05$ and $^{**}p < 0.01$.

nanoparticles incorporated into the nanotubes. The size of the Ag nanoparticles is related to the $AgNO_3$ concentration. The TEM picture acquired from the nanotubes taken from NT-Ag1.0 shown in Fig. 1F demonstrates that the Ag nanoparticles attached to the inner wall of the TiO_2-NTs have a diameter of about 10–20 nm. The AFM images show that the TiO_2-NTs and NT-Ag surfaces have similar roughness values of several hundred nanometers. The AFM image acquired from NT-Ag1.0 (Fig. 1H) is shown here as an example to compare to the TiO_2-NTs (Fig. 1G).

Fig. 2 exhibits the XRD patterns of the specimens. Only peaks corresponding to the anatase phase and Ti substrate can be observed from the TiO_2-NTs. In contrary, Ag peaks appear in the XRD patterns obtained from the NT-Ag samples. In addition, the intensities of the Ag peaks increase from NT-Ag0.5 to NT-Ag2.0, suggesting that the amounts of Ag incorporated into the nanotubes increase with $AgNO_3$ concentrations.

The XPS survey spectra acquired from NT-Ag0.5, NT-Ag1.0, NT-Ag1.5, and NT-Ag2.0 after 5 nm of the surface was sputtered off using Ar^+ bombardment shown in Fig. 3A reveal peaks corresponding to Ti, Ag, O, Ar, and C. The C signal detected by XPS is believed to arise from adventitious contamination. The Ag concentrations determined from the XPS survey spectra of NT-Ag0.5, NT-Ag1.0, NT-Ag1.5, and NT-Ag2.0 are 0.82, 1.24, 1.45, and 1.58 at%, respectively. The XPS depth profile obtained from NT-Ag1.0 in Fig. 3B discloses that Ag is distributed along the entire NT length although the absolute concentration decreases with depth from 1.24 at% near the surface to 0.2 at% at a depth of 3 μm. The high-resolution XPS spectra of Ag obtained from NT-Ag at different depths are shown in Fig. 3C. The binding energies of the Ag 3d peak at 368.25 eV and 374.25 eV can be assigned to $3d_{5/2}$ and $3d_{3/2}$ of metallic Ag^0 [32] and do not shift with depths, indicating that Ag mainly exists in the Ag^0 state in the TiO_2-NTs. SEM, TEM, XRD, and XPS provide unequivocal proof that metallic Ag nanoparticles have been successfully loaded into the TiO_2-NT along the entire length.

3.2. Ag release

Fig. 4A shows the Ag release time profiles from the NT-Ag in PBS.The amounts of released Ag at the various time points follow the order of NT-Ag2.0 > NT-Ag1.5 > NT-Ag1.0 > NT-Ag0.5. Initially, there are relatively large amounts of Ag released into the PBS with NT-Ag2.0 leaching the most, and the amounts of released Ag diminish gradually with immersion time. After two weeks, the amount of released Ag is about one-half of that measured in the first day.

3.3. Antibacterial ability of NT-Ag

The antibacterial effectives against planktonic bacteria in the medium (R*p*) and antibacterial rates for adherent bacteria on the specimens (R*a*) for as long as 30 days are evaluated and the results are shown in Fig. 4B and C, respectively. The TiO_2-NTs have an R*p* value of about 30% which is constant with time. Compared to TiO_2-NTs, the NT-Ag samples have higher R*p* values of about 100% during the first 4 days. The R*p* values of the NT-Ag samples then decrease gradually and that of NT-Ag0.5 diminishes more quickly. After 30 days, the R*p* value of NT-Ag0.5 drops to be about 30% whereas those of the other NT-Ag samples are about 50%. Ag incorporation is effective in preventing bacteria colonization on the specimens throughout the 30 days as illustrated by Fig. 4C. The samples show R*a* values of 100% which do not decrease significantly during this time, with the exception of NT-Ag0.5 which shows a big drop after 10 days reaching a value of about 5% after 30 days. The other three NT-Ag samples still show R*a* values of about 80% up to 30 days.

The ability of the NT-Ag samples to prevent viable bacteria colonization is also verified by fluorescence staining as shown in Fig. 5. After 7 days of repeated bacteria invasion every 24 h, there are large amounts of viable bacteria on the flat Ti and smaller amounts on TiO_2-NTs. In comparison, the amounts of viable bacteria are obviously smaller on the NT-Ag samples and in particular, nearly no viable bacteria can be seen on NT-Ag1.5 and NT-Ag2.0.

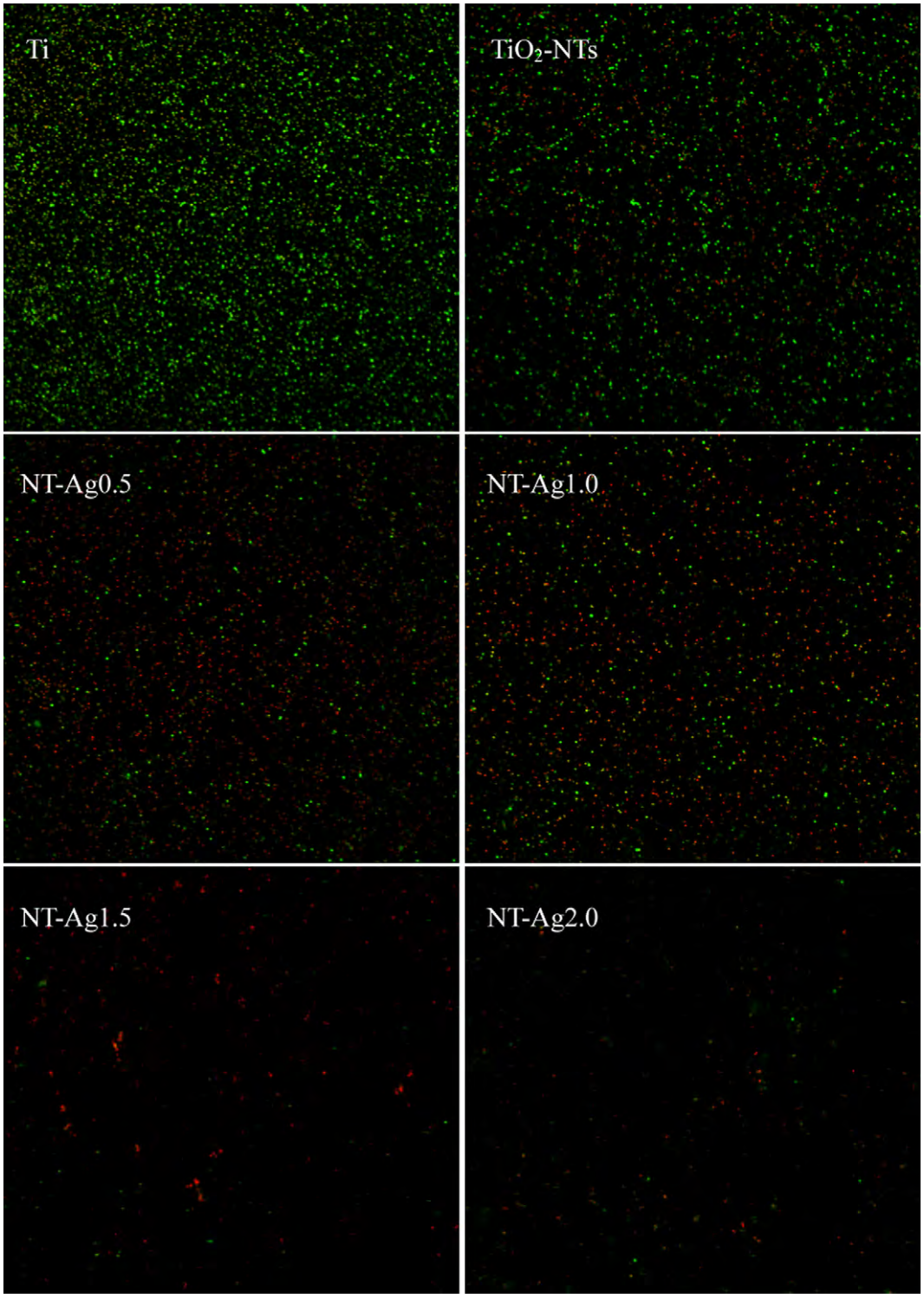

Fig. 5. Representative images showing viability of the bacteria on samples after 7 days of incubation displayed by acridine orange and ethidium bromide fluorescence staining. The live bacteria appear green while dead ones are orange. (For interpretation of the references to colour in this figure legend, the reader is referred to the web version of this article.)

3.4. Protein adsorption

The amounts of adsorbed protein from the 10% bovine calf serum after 4 h of incubation are displayed in Fig. 6. The amounts of proteins on the TiO_2-NTs and NT-Ag samples are more than that on the flat Ti sample. Ag incorporation promotes slightly the protein adsorption ability on TiO_2-NTs but there is no statistical difference among the NT-Ag samples and TiO_2-NTs.

3.5. Cytotoxicity

The cytotoxicity results indicated by the LDH activity in the supernatants after 1 and 4 days of incubation are compared in Fig. 7A. After the first day, neither the TiO_2-NTs nor NT-Ag samples show obvious enhancement in the LDH activity. After culturing for 4 days, NT-Ag0.5, NT-Ag1.0, and NT-Ag1.5 exhibit slightly higher LDH activity than TiO_2-NTs but the difference is statistically

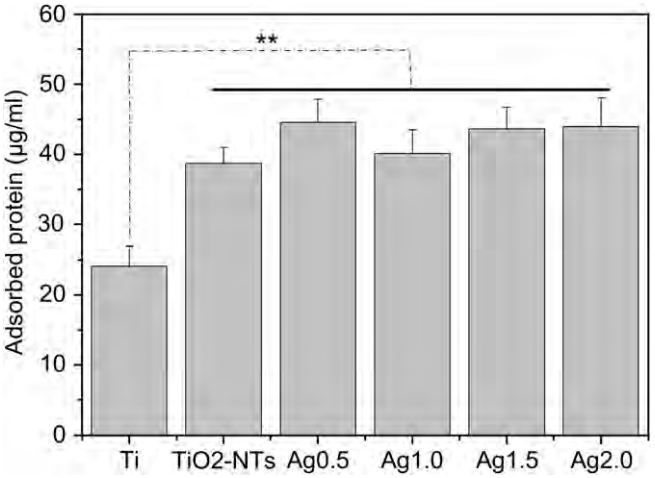

Fig. 6. Amounts of adsorbed protein on different specimens after 4 h of incubation in DMEM containing 10% BCS. The data are expressed as means ± standard deviations ($n = 3$). One-way ANOVA followed by SNK *post hoc* test is utilized to determine the level of significance. $^{**}p < 0.01$.

insignificant. However, higher LDH activity is observed from NT-Ag2.0. Hence, NT-Ag samples exhibit cytotoxicity that is related to the amount of incorporated Ag.

3.6. Cell number

The cell numbers determined by DNA analysis are shown in Fig. 7B. At day 1, there is no appreciable difference on the cell numbers among samples. After 4 days of culturing, the cell number on TiO_2-NTs is smaller than that on flat Ti. Those on the NT-Ag samples are even smaller and the amounts correlate with the silver concentrations.

3.7. Intracellular total protein content and alkaline phosphatase activity

The intracellular total protein synthesis and ALP activity after 7 days of culturing are shown in Fig. 8. The intracellular total protein content and ALP activity on the TiO_2-NTs are similar to those on the flat Ti surface. Addition of Ag decreases the ALP activity and all four NT-Ag samples exhibit dramatically lower ALP activity than the sample without Ag (35–50%). The intracellular total protein synthesis on NT-Ag0.5 and NT-Ag1.0 is similar to that of the TiO_2-NTs but is observed to decrease by 40–60% on NT-Ag1.5 and NT-Ag2.0.

4. Discussion

Infection prevention is a continuous challenge for artificial implants [1] and considering the susceptibility of implant surfaces to biofilm formation and the compromised host defense originating from insufficient osteoconductivity, surface modified Ti with the proper antibacterial ability as well as bio-integration is being actively pursued [33–35]. Long-term antibacterial ability is especially meaningful for implants because of the constant risk of bacterial infection. In this study, NT-Ag coatings are produced on Ti by a simple and economical method that can be readily adopted industrially. In this process, Ag nanoparticles attach to the inner wall along the entire length of the NT. The amount of Ag and size of Ag nanoparticles can be regulated by varying the $AgNO_3$ concentration in the solution and immersion time. In this work, we apply the NT-Ag produced by this method [36] to long-term antibacterial coatings. The NT-Ag surfaces with the proper amount of Ag show

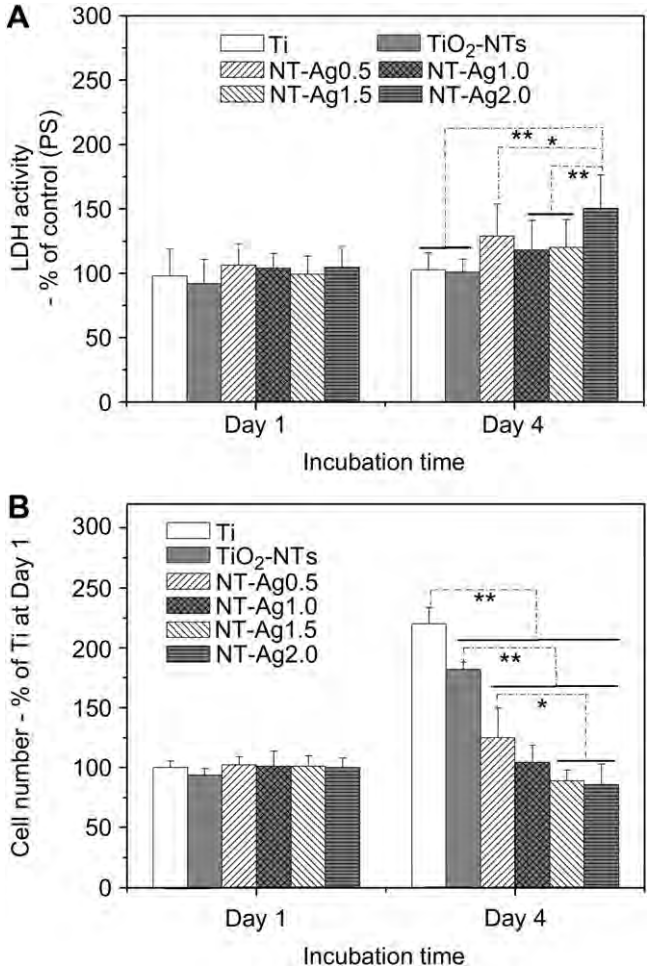

Fig. 7. (A) LDH activity in the culture media and (B) cell numbers determined by DNA assay after osteoblast culturing for 1 and 4 days on the specimens. The data are expressed as means ± standard deviations ($n = 3$). One-way ANOVA followed by SNK *post hoc* test is utilized to determine the level of significance. $^{*}p < 0.05$ and $^{**}p < 0.01$.

relatively long-lasting antibacterial characteristics. This method provides a promising strategy with respect to the fabrication of long-term antibacterial surface while the issue of cytotoxicity can be tackled by controlling the Ag release rate. The long-term bacterial resistance demonstrated here is especially effective in preventing implant associated infection both in the early and medium stage.

Although antibacterial coatings have been researched extensively, it is still a challenge to produce one with relatively long-lasting antibacterial effects. Theoretically, non-leaching and anti-adherent coatings with the proper surface structure may possess persistent antibacterial ability to prevent biofilm formation. Unfortunately, the efficacy of anti-adherent coatings in reducing bacterial adhesion is typically limited and varies greatly depending on the bacteria species. Moreover, these coatings are prone to degradation in the physiological environment. In contrast, more sturdy coatings loaded with an antibacterial agent can provide more preannounced antibacterial effects [1]. However, the limited capacity of most coatings cannot yield long-term antibacterial effects via the normal mechanism of antibiotics loading and releasing, and so there have been attempts to covalently bond antibiotics to the materials [37]. However, as a protein layer will quickly deposit on the implant under physiological conditions, it is highly questionable if the covalently bonded antibiotics can

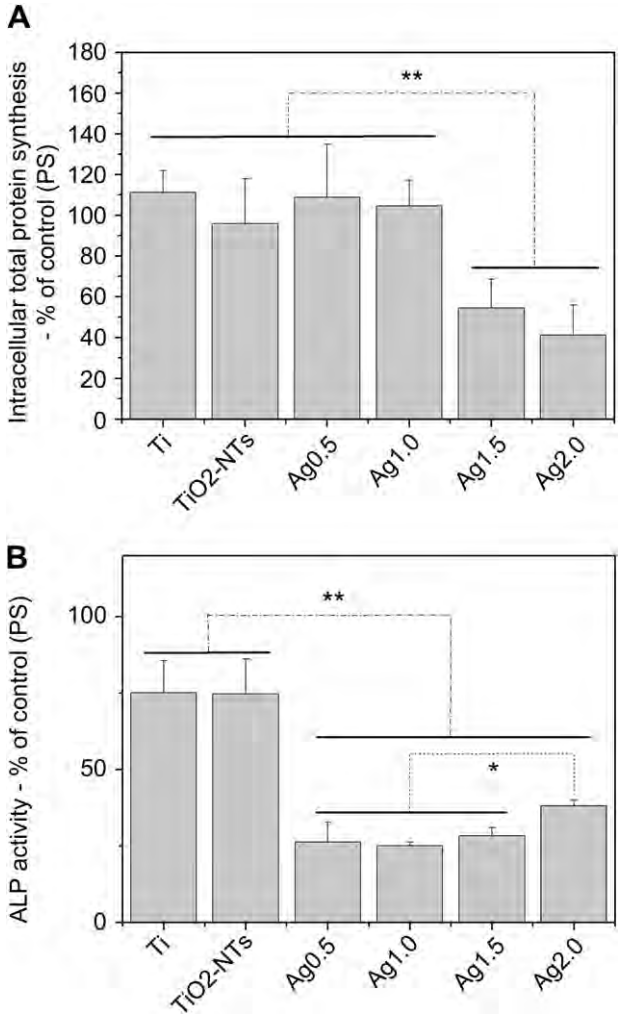

Fig. 8. (A) Intracellular total protein synthesis and (B) ALP activity of osteoblasts on the specimens after incubation for 7 days. The data are expressed as means ± standard deviations ($n = 3$). One-way ANOVA followed by SNK *post hoc* test is utilized to determine the level of significance. $^{*}p < 0.05$ and $^{**}p < 0.01$.

penetrate this protein layer. Besides, the development of new antibiotics resistance deters potential clinical applications of antibiotics loaded coatings. Immobilization of antimicrobial peptides which are safer than antibiotics has drawn interest [38,39]. However, this concept suffers from the same drawback as covalently bonded antibiotics with regard to penetration through this protein layer. In addition, although the immobilized peptides may withstand some harsh procedures [38], they decompose gradually *in vivo* thereby seriously affecting the long-term effects. In comparison, a coating doped with a proper amount of Ag can potentially yield long-lasting antibacterial effects and one example is the NT-Ag structure reported here for the following reasons. First of all, the biocompatibility of the NT-Ag can be tailored based on many previous studies on the biological properties of TiO_2-NTs and Ag [1,3,24,25]. Secondly, the difficulty for bacteria to develop resistance against this element bodes well for *in vivo* applications [40]. Thirdly, the high efficacy of Ag at very low concentrations and relatively large reservoir provided by the nanotubes can give rise to long-term antibacterial effects. Fourthly, the stability of the NT-Ag in the physiological environment is excellent due to its inorganic nature, and last but not least, the fabricating process for NT-Ag is easy, economical, and suitable for industrial production.

The NT-Ag surfaces show excellent antibacterial ability throughout the 30 day period. All the planktonic bacteria in the medium are killed during the first several days, but it should be noted that the efficacy diminishes gradually with time as a result of the Ag release profile with time. Initially, a large amount of Ag is released but it diminishes gradually with immersion time. The large initial Ag release may stem from the Ag nanoparticles on the surface of the nanotubes which oxidize when reacting with water. Nonetheless, with the exception of NT-Ag0.5 which has the lowest silver concentration, the ability of the other samples to prevent bacterial adhesion on the Ti implant lasts for the whole month without too much reduction. These antibacterial properties are very meaningful to clinical applications. The initial phase after implantation is the most dangerous and prone to infection, and so the strong ability of NT-Ag to kill surrounding planktonic bacteria helps prevent post-operation infection and guarantee normal wound healing in the early stage. After this period, since the surgery site has achieved primary healing and osseointegration will be completed gradually with time, inhibition of bacterial adhesion and biofilm formation through a low level Ag release mechanism is sufficient to prevent later-stage infection conjugated with the host defense. Hence the Ag release profile and rate meets clinical requirements.

Although longer term studies up to 6 months to perhaps 2 years should be conducted in the next stage of clinical trials to demonstrate the viability, the effective period in which NT-Ag can resist bacteria adhesion is expected to be longer than the 30 days experimentally demonstrated here. It is worth mentioning that in our antibacterial assay, the samples are subject to intense bacteria attack by immersing in 1 ml of the bacteria suspension containing 10^5 CFU/ml and changing the bacteria suspension daily. These conditions are much harsher than the normal situation *in vivo*. Consequently, the samples that show excellent antibacterial ability during the first 30 days are expected to be good for a much longer period of time under normal conditions. Even though Humblot et al. [39] reported that their antibacterial peptide Magainin I covalently bound coatings exhibited activity up to six months, their coatings were actually only subjected to a total of four bacteria attacks (initial assay and assays after one week, one month, and six months) and were incubated for only 3 h each time. Hence, the severity of their bacterial challenge is far less than that in the present study. Besides, the Magainin I covalently bound coatings have an inhibition rate of 60–70% and show obvious decline in the fourth assay. Therefore, our NT-Ag samples produce stronger and more long-lasting antibacterial effects than the Magainin I immobilized coatings. Release of biologically active Ag from the NT-Ag is related to the aqueous reaction in which the Ag nanoparticles form Ag^+ [41]. As water infiltrates the nanotubes, the surface of the nanoparticles is oxidized to release Ag^+ (Fig. 9A). As the NT-Ag is loaded with Ag along the entire depth of NTs and infiltration of body fluids into the nanotubes is slow, slow Ag^+ release and consequently long-term bacteria resistance are expected.

Ag is generally regarded to be cytocompatible at low concentrations, but high doses of Ag can induce cytotoxicity leading to safety concerns [28,29]. In this study, the NT-Ag samples are ultrasonically cleaned to remove loosely adhered Ag nanoparticles and adsorbed Ag^+ to avoid excessive Ag^+ release in the early stage. Nonetheless, the NT-Ag surfaces still show some cytotoxicity as demonstrated by the higher level of LDH in the culture medium compared to the control after 4 days of culture, especially NT-Ag2.0 which has the largest concentration of Ag. The cytotoxicity of the NT-Ag surfaces is also verified by the DNA content assay, intracellular total protein content, and early differentiation marker ALP activity, which are also depressed by Ag incorporation with the extent depending on the Ag concentration. The cytotoxicity of the

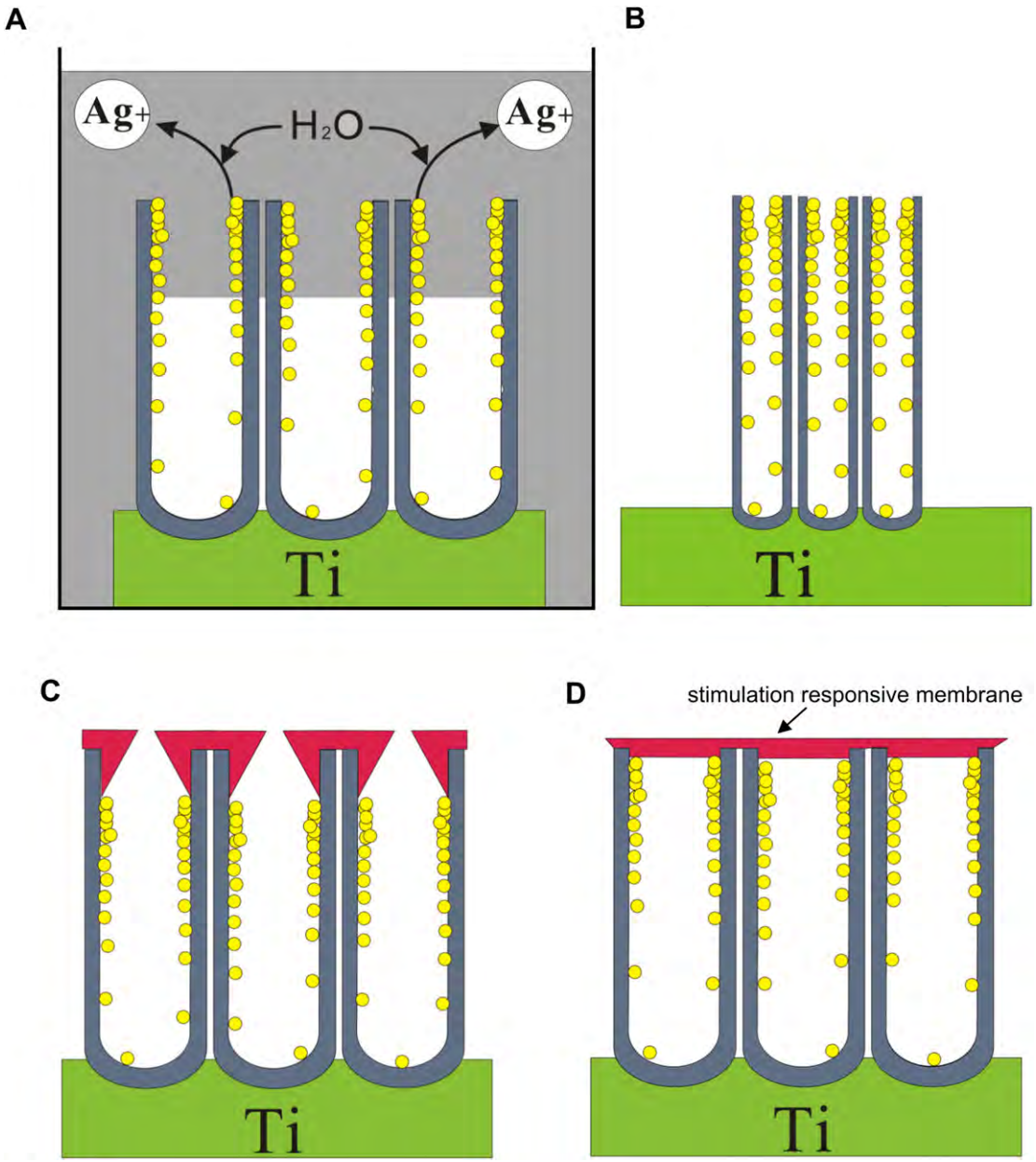

Fig. 9. (A) Schematic diagram shows the mechanism of antibacterial ability of NT-Ag under aqueous conditions. As water gradually infiltrates the nanotubes, the surface of the nanoparticles is oxidized to release Ag^+. (B) Use of nanotubes with a smaller size may lead to slower water infiltration and Ag^+ release. (C) The openings of the nanotubes can be shrunk by depositing another coating such as hydroxyapatite or polymer to control water infiltration and Ag^+ release. (D) Stimulation responsive membranes may be utilized to produce smart antibacterial coatings that deliver bactericides on demand.

NT-Ag surfaces can be attributed to rapid leaching of Ag^+ and accumulation in the culture medium. It can be observed that at day 1, the NT-Ag surfaces show no obvious cytotoxicity. As the culture medium is not changed until the third day, the cumulative concentration of leached Ag^+ leads to obvious cytotoxicity at day 4. Experimental evidence shows that biomaterials containing a proper amount of Ag are compatible to mammalian cells including osteoblasts [3,24,26,28,29] and it has been suggested that some Ag-containing coatings even enhance osteoblast proliferation [25,42] and fibroblast attachment and endothelial cell response [43]. Therefore, we believe that by properly controlling the silver release rate, NT-Ag with good cytocompatiblity can be produced.

The rate of Ag^+ leaching from the NT-Ag samples may be controlled by several strategies in order to reduce the cytotoxicity and simultaneously prolong the antibacterial time. The diameter of the TiO_2-NTs in this study is 130 nm which facilitates infiltration of water leading to fast leaching of Ag^+ and subsequent cytotoxicity. There is evidence that drug elution from TiO_2-NTs can be controlled by the tube dimension [44]. Since the size of the TiO_2-NTs can be varied from tens to hundreds of nanometers by adjusting the anodization parameters, the most direct method to accomplish controlled release of Ag^+ is to select TiO_2-NTs with a size smaller than 130 nm which should reduce water infiltration and Ag^+ release (Fig. 9B). Furthermore, the release of biologically active Ag from the Ag nanoparticles can be controlled by changing the oxidation reactions in water. It has been reported that a variety of competing chemical approaches can accomplish this purpose [45] and they may be applied to control Ag^+ release from the Ag nanoparticles in NT-Ag. The openings of the nanotubes can also be shrunk by another coating after Ag incorporation in order to control

the Ag^+ leaching rate (Fig. 9C). A simple and direct method is deposition of hydroxyapatite in simulated body fluids. The nanotubular structure can induce hydroxyapatite deposition [13] and by choosing the suitable simulated body fluid and controlling the immersion time, the tube openings can be moderately narrowed [46]. The openings of the nanotubes can be reduced significantly or even completely closed by a thin and chemically reactive polymer produced by plasma polymerization. This provides the basis for further surface functionalization by attaching desirable molecules [47]. Smart coatings which deliver bactericidal agents only when bacteria invasion occurs are ideal, because a longer antibacterial period can be achieved and side effects caused by long-term bactericidal agent delivery can be circumvented simultaneously. There are many stimulation responsive biomaterials such as pH-sensitive, temperature-sensitive and electric-signal-sensitive hydrogels [48] which may be applied to the openings of the nanotubes loaded with Ag as an "on-off" switch to control Ag^+ release on demand, but it is a big challenge to do so properly and reliably (Fig. 9D). Drug release triggered by bacterial toxin from gold nanoparticle-stabilized liposomes has recently been reported [49] demonstrating hopeful realization of long-term smart antibacterial coatings encompassing the NT-Ag structure.

Besides controlling Ag leaching, the technique described in this paper can be improved to incorporate a larger amount of Ag into the TiO_2-NTs. Parameters such as the $AgNO_3$ concentration, additives, and immersion time can be further optimized and ultrasonic treatment may be utilized to facilitate $AgNO_3$ infiltration and increase the amount of incorporated Ag. Besides, nanotubes with a bigger size can be used and it may be of interest to try other Ag loading methods. Macak et al. have reported that TiO_2-NTs can be filled with copper by a self-doping and electro-deposition technique [50] which may be extended to load TiO_2-NTs with Ag. We are performing some of these experiments in our laboratory and additional findings will be reported in due course.

5. Conclusion

In summary, Ag nanoparticles are incorporated into TiO_2-NTs on Ti implants using a simple procedure involving $AgNO_3$ immersion and UV irradiation. The Ag nanoparticles adhere strongly to the inner walls of the nanotubes along the entire length, and the size and amount of Ag nanoparticles can be regulated by adjusting the $AgNO_3$ concentration and immersion time. The NT-Ag possesses the ability to kill all the planktonic bacteria in the culture medium during the first several days and the capability to prevent bacterial adhesion is maintained for 30 days, with the exception of NT-Ag0.5 which has the smallest Ag concentration. Since the conditions used in our experiments are more severe than those encountered normally *in vivo*, the materials are expected to be effective for a much longer time in the normal situation. This relatively long-term effect bodes well for prevention of initial and intermediate-stage infection after operation and perhaps even late infection. Although the NT-Ag samples show some cytotoxicity, it can be reduced by controlling the Ag release rate and the properties can be further tailored to accomplish both long-term antibacterial ability and biointegration. The materials are thus very attractive for biomedical implants due to prevention of implant associated infection and promotion of osseointegration.

Acknowledgments

This work was jointly supported by National High Technology Research and Development Program of China No. 2009AA02Z416, National Natural Science Foundation of China No. 50902104 and 81070862, Hubei Province Natural Science Foundation No.2010CDB03402, City University of Hong Kong Strategic Research Grant (SRG) No. 7008009, and Hong Kong Research Grants Council (RGC) General Research Funds (GRF) No. CityU 112510.

References

[1] Zhao L, Chu PK, Zhang Y, Wu Z. Antibacterial coatings on titanium implants. J Biomed Mater Res B Appl Biomater 2009;91:470–80.
[2] Darouiche RO. Treatment of infections associated with surgical implants. N Engl J Med 2004;350:1422–9.
[3] Hardes J, Ahrens H, Gebert C, Streitbuerger A, Buerger H, Erren M, et al. Lack of toxicological side-effects in silver-coated megaprostheses in humans. Biomaterials 2007;28:2869–75.
[4] Schmalzried TP, Amstutz HC, Au MK, Dorey FJ. Etiology of deep sepsis in total hip arthrosplasty. The significance of hematogenous and recurrent infections. Clin Orthop Rel Res 1992;280:200–7.
[5] Green SA, Ripley MJ. Chronic osteomyelitis in pin tracks. J Bone Jt Surg Am 1984;66:1092–8.
[6] Monteiro DR, Gorup LF, Takamiya AS, Ruvollo-Filho AC, de Camargo ER, Barbosa DB. The growing importance of materials that prevent microbial adhesion: antimicrobial effect of medical devices containing silver. Int J Antimicrob Agents 2009;34:103–10.
[7] Mah TF, O'Toole GA. Mechanisms of biofilm resistance to antimicrobial agents. Trends Microbiol 2001;9:34–9.
[8] Webster TJ, Ejiofor JU. Increased osteoblast adhesion on nanophase metals: Ti, Ti6Al4V, and CoCrMo. Biomaterials 2004;25:4731–9.
[9] Hajicharalambous CS, Lichter J, Hix WT, Swierczewska M, Rubner MF, Rajagopalan P. Nano- and sub-micron porous polyelectrolyte multilayer assemblies: biomimetic surfaces for human corneal epithelial cells. Biomaterials 2009;30:4029–36.
[10] Mendonca G, Mendonca DB, Aragao FJ, Cooper LF. Advancing dental implant surface technology–from micron- to nanotopography. Biomaterials 2008;29:3822–35.
[11] Zhao L, Mei S, Chu PK, Zhang Y, Wu Z. The influence of hierarchical hybrid micro/nano-textured titanium surface with titania nanotubes on osteoblast functions. Biomaterials 2010;31:5072–82.
[12] Zhao L, Mei S, Wang W, Chu PK, Wu Z, Zhang Y. The role of sterilization in the cytocompatibility of titania nanotubes. Biomaterials 2010;31:2055–63.
[13] Oh SH, Finones RR, Daraio C, Chen LH, Jin S. Growth of nano-scale hydroxyapatite using chemically treated titanium oxide nanotubes. Biomaterials 2005;26:4938–43.
[14] Oh S, Daraio C, Chen LH, Pisanic TR, Finones RR, Jin S. Significantly accelerated osteoblast cell growth on aligned TiO_2 nanotubes. J Biomed Mater Res Part A 2006;78:97–103.
[15] Brammer KS, Oh S, Cobb CJ, Bjursten LM, van der Heyde H, Jin S. Improved bone-forming functionality on diameter-controlled TiO_2 nanotube surface. Acta Biomater 2009;5:3215–23.
[16] Das K, Bose S, Bandyopadhyay A. TiO_2 nanotubes on Ti: influence of nanoscale morphology on bone cell-materials interaction. J Biomed Mater Res A 2009;90:225–37.
[17] Crawford GA, Chawla N, Das K, Bose S, Bandyopadhyay A. Microstructure and deformation behavior of biocompatible TiO_2 nanotubes on titanium substrate. Acta Biomater 2007;3:359–67.
[18] Popat KC, Eltgroth M, Latempa TJ, Grimes CA, Desai TA. Decreased Staphylococcus epidermis adhesion and increased osteoblast functionality on antibiotic-loaded titania nanotubes. Biomaterials 2007;28:4880–8.
[19] Eaninwene 2nd G, Yao C, Webster TJ. Enhanced osteoblast adhesion to drug-coated anodized nanotubular titanium surfaces. Int J Nanomedicine 2008;3:257–64.
[20] Campoccia D, Montanaro L, Arciola CR. The significance of infection related to orthopedic devices and issues of antibiotic resistance. Biomaterials 2006;27:2331–9.
[21] Arciola CR, Campoccia D, Gamberini S, Donati ME, Pirini V, Visai L, et al. Antibiotic resistance in exopolysaccharide-forming Staphylococcus epidermidis clinical isolates from orthopaedic implant infections. Biomaterials 2005;26:6530–5.
[22] Arciola CR, Baldassarri L, Campoccia D, Creti R, Pirini V, Huebner J, et al. Strong biofilm production, antibiotic multi-resistance and high gelE expression in epidemic clones of Enterococcus faecalis from orthopaedic implant infections. Biomaterials 2008;29:580–6.
[23] Hendriks JG, van Horn JR, van der Mei HC, Busscher HJ. Backgrounds of antibiotic-loaded bone cement and prosthesis-related infection. Biomaterials 2004;25:545–56.
[24] Alt V, Bechert T, Steinrucke P, Wagener M, Seidel P, Dingeldein E, et al. An in vitro assessment of the antibacterial properties and cytotoxicity of nanoparticulate silver bone cement. Biomaterials 2004;25:4383–91.
[25] Bosetti M, Masse A, Tobin E, Cannas M. Silver coated materials for external fixation devices: in vitro biocompatibility and genotoxicity. Biomaterials 2002;23:887–92.
[26] Chen W, Liu Y, Courtney HS, Bettenga M, Agrawal CM, Bumgardner JD, et al. In vitro anti-bacterial and biological properties of magnetron co-sputtered silver-containing hydroxyapatite coating. Biomaterials 2006;27:5512–7.

[27] Necula BS, Fratila-Apachitei LE, Zaat SA, Apachitei I, Duszczyk J. In vitro antibacterial activity of porous TiO_2-Ag composite layers against methicillin-resistant Staphylococcus aureus. Acta Biomater 2009;5:3573–80.
[28] Agarwal A, Weis TL, Schurr MJ, Faith NG, Czuprynski CJ, McAnulty JF, et al. Surfaces modified with nanometer-thick silver-impregnated polymeric films that kill bacteria but support growth of mammalian cells. Biomaterials 2010; 31:680–90.
[29] Ramstedt M, Ekstrand-Hammarstrom B, Shchukarev AV, Bucht A, Osterlund L, Welch M, et al. Bacterial and mammalian cell response to poly(3-sulfopropyl methacrylate) brushes loaded with silver halide salts. Biomaterials 2009;30: 1524–31.
[30] Zhao L, Wei Y, Li J, Han Y, Ye R, Zhang Y. Initial osteoblast functions on Ti-5Zr-3Sn-5Mo-15Nb titanium alloy surfaces modified by microarc oxidation. J Biomed Mater Res A 2010;92:432–40.
[31] Cui L, Liu B, Liu G, Zhang W, Cen L, Sun J, et al. Repair of cranial bone defects with adipose derived stem cells and coral scaffold in a canine model. Biomaterials 2007;28:5477–86.
[32] Jin M, Zhang X, Nishimoto S, Liu Z, Tryk DA, Emeline AV, et al. Light-stimulated composition conversion in TiO_2-based nanofibers. J Phys Chem C 2007;111: 658–65.
[33] Chua PH, Neoh KG, Kang ET, Wang W. Surface functionalization of titanium with hyaluronic acid/chitosan polyelectrolyte multilayers and RGD for promoting osteoblast functions and inhibiting bacterial adhesion. Biomaterials 2008;29:1412–21.
[34] Zhang F, Zhang Z, Zhu X, Kang ET, Neoh KG. Silk-functionalized titanium surfaces for enhancing osteoblast functions and reducing bacterial adhesion. Biomaterials 2008;29:4751–9.
[35] Harris LG, Tosatti S, Wieland M, Textor M, Richards RG. Staphylococcus aureus adhesion to titanium oxide surfaces coated with non-functionalized and peptide-functionalized poly(L-lysine)-grafted-poly(ethylene glycol) copolymers. Biomaterials 2004;25:4135–48.
[36] Paramasivam I, Macak JM, Ghicov A, Schmuki P. Enhanced photochromism of Ag loaded self-organized TiO_2 nanotube layers. Chem Phys Lett 2007;445: 233–7.
[37] Antoci Jr V, Adams CS, Parvizi J, Davidson HM, Composto RJ, Freeman TA, et al. The inhibition of Staphylococcus epidermidis biofilm formation by vancomycin-modified titanium alloy and implications for the treatment of periprosthetic infection. Biomaterials 2008;29:4684–90.
[38] Costa F, Carvalho IF, Montelaro RC, Gomes P, Martins MC. Covalent immobilization of antimicrobial peptides (AMPs) onto biomaterial surfaces. Acta Biomater 2011;7:1431–40.
[39] Humblot V, Yala JF, Thebault P, Boukerma K, Hequet A, Berjeaud JM, et al. The antibacterial activity of Magainin I immobilized onto mixed thiols Self-Assembled Monolayers. Biomaterials 2009;30:3503–12.
[40] Percival SL, Bowler PG, Russell D. Bacterial resistance to silver in wound care. J Hosp Infect 2005;60:1–7.
[41] Kumar R, Howdle S, Munstedt H. Polyamide/silver antimicrobials: effect of filler types on the silver ion release. J Biomed Mater Res B Appl Biomater 2005;75:311–9.
[42] Verne E, Di Nunzio S, Bosetti M, Appendino P, Brovarone CV, Maina G, et al. Surface characterization of silver-doped bioactive glass. Biomaterials 2005;26:5111–9.
[43] Hsu SH, Tseng HJ, Lin YC. The biocompatibility and antibacterial properties of waterborne polyurethane-silver nanocomposites. Biomaterials 2010;31: 6796–808.
[44] Peng L, Mendelsohn AD, LaTempa TJ, Yoriya S, Grimes CA, Desai TA. Long-term small molecule and protein elution from TiO_2 nanotubes. Nano Lett 2009;9: 1932–6.
[45] Liu J, Sonshine DA, Shervani S, Hurt RH. Controlled release of biologically active silver from nanosilver surfaces. ACS Nano 2010;4:6903–13.
[46] Dey T, Roy P, Fabry B, Schmuki P. Anodic mesoporous TiO_2 layer on Ti for enhanced formation of biomimetic hydroxyapatite. Acta Biomater 2011;7: 1873–9.
[47] Vasilev K, Poh Z, Kant K, Chan J, Michelmore A, Losic D. Tailoring the surface functionalities of titania nanotube arrays. Biomaterials 2010;31:532–40.
[48] Qiu Y, Park K. Environment-sensitive hydrogels for drug delivery. Adv Drug Deliv Rev 2001;53:321–39.
[49] Pornpattananangkul D, Zhang L, Olson S, Aryal S, Obonyo M, Vecchio K, et al. Bacterial toxin-triggered drug release from gold nanoparticle-stabilized liposomes for the treatment of bacterial infection. J Am Chem Soc 2011; 133:4132–9.
[50] Macak JM, Gong BG, Hueppe M, Schmuki P. Filling of TiO_2 nanotubes by self-doping and Electrodeposition. Adv Mater 2007;19:3027–31.